$K_{3+\delta}C_{84}$. Higher Fullerene Analogues of the A_3C_{60} Superconductors

M. S. Denning,[†] T. J. S. Dennis,[‡] M. J. Rosseinsky,*[,§] and H. Shinohara[||]

Inorganic Chemistry Laboratory, University of Oxford, South Parks Road, Oxford OX1 3QR, United Kingdom, Department of Chemistry, Queen Mary and Westfield College, University of London, Mile End Road, London E1 4NS, United Kingdom, Department of Chemistry, University of Liverpool, Liverpool L69 7ZD, United Kingdom, and Department of Chemistry, Nagoya University, Nagoya 464-8602, Japan

Received June 21, 2001. Revised Manuscript Received August 14, 2001

Face-centered cubic phases of both the D_2 and D_{2d} isomers of the C_{84} anion with band fillings close to those of the A_3C_{60} superconductors are prepared by a two-step reaction involving saturated $K_{8+x}C_{84}$ phases as intermediates. Rietveld refinement shows that the structures are more disordered than those of $K_{8+x}C_{84}$, with incomplete occupancy of multiple cation sites and the presence of two anion orientations, while both temperature-dependent powder diffraction and EPR demonstrate the monophasic nature of the reaction products. The temperature-independent magnetic susceptibilities and line width variation in EPR indicate that these phases have finite densities of states at the Fermi level for both C_{84} majority isomers, unlike the previously prepared saturated phases, but dc magnetization measurements indicate the absence of superconductivity above 5 K.

Introduction

The electronic properties of fullerene solids are extremely sensitive to the molecular symmetry and charge state, a fact best demonstrated by the A_3C_{60} superconductors.[1,2] Cubic A_3C_{60} phases are both metallic and superconducting, but deviation of the charge from 3−[3,4] (corresponding to half-filling of the band derived from the t_{1u} LUMO) or reduction of the symmetry[5,6] suppresses first superconductivity and then metallic behavior. Orthorhombic $(NH_3)K_3C_{60}$ is an itinerant electron system undergoing an antiferromagnetic metal−insulator transition below 40 K,[7] although cubic A_3C_{60} systems with greater inter-C_{60} distances[8] remain metallic and superconducting. This complex relationship between structure, charge and electronic behavior is less well-explored for other charge states, but interesting properties have emerged from the limited studies thus far: the C_{60}^{8-} (Sr_4C_{60})[9] and C_{60}^{9-} ($K_3Ba_3C_{60}$)[10] t_{1g} superconductors have a dependence of T_c on pressure opposite that of the A_3C_{60} phases, while counterion-free oxidation of C_{60} in a field-effect transistor produces superconductivity over a wide range of hole concentrations with a maximum T_c of 52 K.[11]

Combined structural and electronic property measurements are required to reveal the details of the intercalation chemistry and structure−charge−property relationships in fullerenes other than C_{60}, and due to experimental difficulties in handling the small quantities available of these materials, there has been little progress in this area until recently. Theoretical work indicates that doped derivatives of non-C_{60} fullerenes (such as C_{28} and C_{36}) should have superconducting properties superior to those of the A_3C_{60} phases due to the enhanced hybridization of the π-symmetry orbitals with increased curvature of the fullerene cage.[12] At present, detailed structural and electronic information is available only for $K_{8+x}C_{84}$[13] and Sm_3C_{70},[14] which have compositions close to those of filled band insulators and do not have the magnetic or (in the C_{70} case) transport properties of metals.

C_{70} is the most abundant higher fullerene, but its ellipsoidal shape mitigates strongly against the adoption of the partially orientationally ordered structures characteristic of the A_3C_{60} superconductors. The most abun-

* To whom correspondence should be addressed.
[†] University of Oxford.
[‡] University of London.
[§] University of Liverpool.
[||] Nagoya University.

(1) Rosseinsky, M. J. *Chem. Mater.* **1998**, *10*, 2665−2685.
(2) Prassides, K. *Curr. Opin. Solid State Mater. Sci.* **1997**, *2*, 433−439.
(3) Kosaka, M.; Tanigaki, K.; Prassides, K.; Margadonna, S.; Lappas, A.; Brown, C. M.; Fitch, A. N. *Phys. Rev. B* **1999**, *59*, R6628−R6630.
(4) Yildirim, T.; Barbedette, L.; Fischer, J. E.; Lin, C. L.; Robert, J.; Petit, P.; Palstra, T. T. M. *Phys. Rev. Lett.* **1996**, *77*, 167−170.
(5) Rosseinsky, M. J.; Murphy, D. W.; Fleming, R. M.; Zhou, O. *Nature* **1993**, *364*, 425−427.
(6) Takenobu, T.; Muro, T.; Iwasa, Y.; Mitani, T. *Phys. Rev. Lett.* **2000**, *85*, 381.
(7) Prassides, K.; Margadonna, S.; Arcon, D.; Lappas, A.; Shimoda, H.; Iwasa, Y. *J. Am. Chem. Soc.* **1999**, *121*, 11227−11228.
(8) Dahlke, P.; Denning, M. S.; Henry, P. F.; Rosseinsky, M. J. *J. Am. Chem. Soc.* **2000**, *122*, 12352−12361.
(9) Brown, C. M.; Taga, S.; Gogia, B.; Kordatos, K.; Margadonna, S.; Prassides, K.; Iwasa, Y.; Tanigaki, K.; Fitch, A. N.; Pattison, P. *Phys. Rev. Lett.* **1999**, *83*, 2258−2261.
(10) Iwasa, Y.; Kawaguchi, M.; Iwasaki, H.; Mitani, T.; Wada, N.; Hasegawa, T. *Phys. Rev. B: Condens. Matter* **1998**, *57*, 13395−13398.
(11) Schon, J. H.; Kloc, C.; Batlogg, B. *Nature* **2000**, *408*, 549−552.
(12) Breda, N.; Broglia, R. A.; Colo, G.; Onida, G.; Provasi, D.; Vigezzi, E. *Phys. Rev. B* **2000**, *62*, 130.
(13) Allen, K. M.; Dennis, T. J. S.; Rosseinsky, M. J.; Shinohara, H. *J. Am. Chem. Soc.* **1998**, *120*, 6681−6689.
(14) Chen, X. H.; Chi, D. H.; Sun, Z.; Takenobu, T.; Liu, Z. S.; Iwasa, Y. *J. Am. Chem. Soc.* **2000**, *122*, 5729−5732.

10.1021/cm010595c CCC: $20.00
Published on Web 10/09/2001

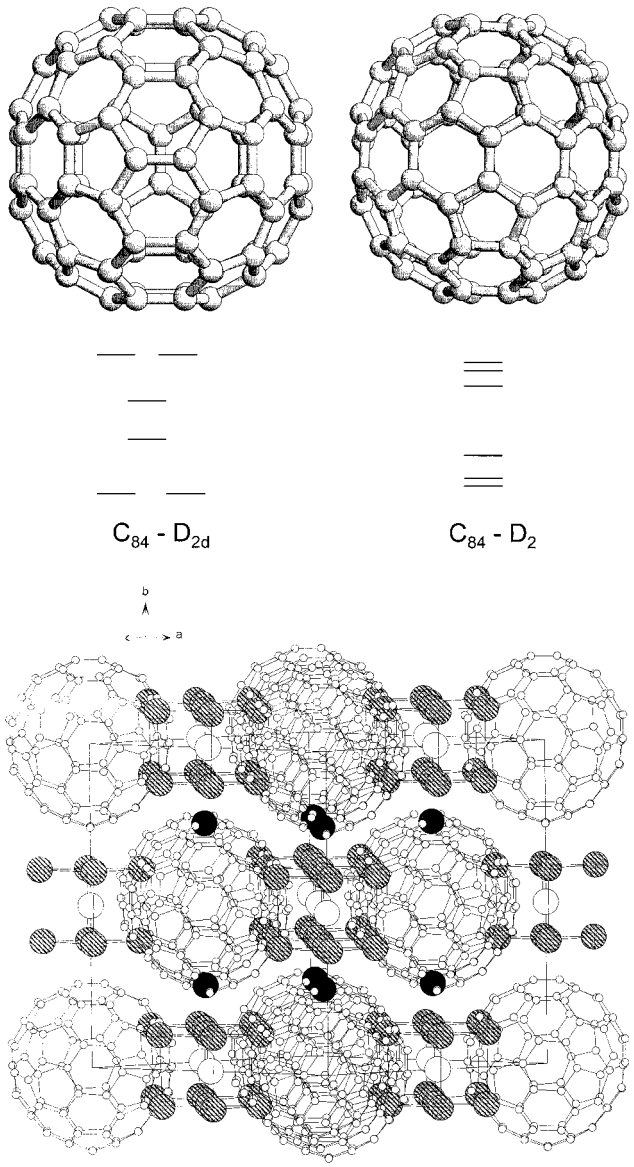

Figure 1. (a, top) The two majority isomers of C_{84} and their lowest unoccupied molecular orbitals. The orbital energies are drawn to scale with extended Hückel calculations. (b, bottom) Crystal structure of $K_{8+x}C_{84}$ showing the occupancy of the octahedral (white) and tetrahedral (black) cation sites found in K_3C_{60} plus the cube of cations (gray hatched) centered around the octahedral site.

dant D_2 and D_{2d} isomers of C_{84} have near spherical symmetry (Figure 1a) and, unlike the rhombohedral and monoclinic modifications of C_{70}, adopt face-centered cubic (fcc) structures at room temperature.[15] This, combined with the doubly degenerate C_{84} LUMO, gives the intercalation chemistry of C_{84} particular interest.

Ultraviolet photoelectron spectra and conductivity measurements of K_xC_{84} films prepared by intercalation into mixed-isomer solids have been reported as a function of the doping level,[16] showing conductivities of up to 1 S cm^{-1} at $x = 6$, but with vanishing densities of states at the Fermi level at all compositions.

The only previous isomer-pure intercalation chemistry of C_{84}[13] demonstrated that reaction with excess potassium produced fcc phases with a stoichiometry of $K_{8+x}C_{84}$, in which there was multiple occupancy of the octahedral site by potassium and partial orientational ordering of the C_{84} anions (Figure 1b). Although the multiple potassium occupancy of the octahedral site can be interpreted in terms of cubic K_8 units, EPR and inter-potassium contact distance evidence indicates complete charge transfer to the fullerene and the absence of significant K···K bonding. The C_{84}-based electrons are clearly localized in 2:1 mixed-isomer and D_2 C_{84} saturated phases, but the susceptibility data on D_{2d} $K_{8.39}C_{84}$ indicate strong spin−spin coupling.

In this paper we investigate the synthesis of K_xC_{84} phases with less than saturation metal doping, using a two-step synthesis procedure to ensure lower band fillings, and demonstrate metallic but not superconducting behavior in these phases, which have structures closely related to that of K_3C_{60}. This represents the first step in delineating the charge−structure−property relationships for higher fullerides.

Experimental Section

Isomer-pure D_{2d} and D_2 C_{84} samples were prepared by the recycling HPLC procedure described previously.[17] The resulting CS_2-solvated C_{84} was dissolved in benzene and transferred to a small Pyrex insert to allow the removal of solvent by evaporation under a flow of nitrogen, followed by heating to 160 °C at a pressure of 10^{-5} Torr for 8 h. The C_{84}-containing insert was then sealed in a 9 mm Pyrex tube together with an excess of potassium metal, as described by Allen et al.,[13] and treated at 250 °C (with the fullerene-containing portion of the tube at the hot end of a 10 °C temperature gradient to prevent condensation of potassium onto the fullerene). The product of this reaction, assumed to be K_8C_{84}, was then combined with pristine C_{84} to produce a nominal composition, K_2C_{84}. The refined compositions differ substantially from this value, as detailed later, which is attributed to excess potassium condensed onto the surface of the $K_{8+x}C_{84}$ during the cooling from 250 °C as well as insertion of potassium into the $K_{8+x}C_{84}$ phase above the values found by Allen et al. The samples were heated to 250 °C for 6 h and 300 °C for a further 12 h before being ground thoroughly in the drybox and resealed. The reground samples were then heated at 350 °C for 48 h.

Preliminary X-ray powder diffraction data were recorded on a Siemens D5000 diffractometer with Cu $K\alpha_1$ radiation and a linear position-sensitive detector. Data for structure analysis at ambient temperature were recorded on the BM16 X-ray powder diffractometer at the European Synchrotron Radiation Facility (ESRF) at a wavelength of 0.83500(1) Å calibrated with NBS silicon. Diffraction patterns at temperatures of up to 623 K were recorded on station 9.1 of the Synchrotron Radiation Source, Daresbury Laboratory, at wavelengths of 0.99856(1) and 0.998155(1) Å. Data were analyzed with the Rietveld method using the GSAS software. EPR data were collected on 0.6 mg samples sealed in quartz capillaries using a Varian E-line spectrometer at a microwave frequency of 9.23 GHz between 5 and 300 K. *g* values were calibrated with a DPPH standard, and the magnetic susceptibility was calibrated using K_3C_{60}, whose susceptibility was taken to be 8.5×10^{-4} emu mol^{-1}. Power levels for the measurements were selected from power-dependent measurements at 4.2 K to avoid saturation effects: 0.04 mW was used in both cases. dc magnetization data were recorded on a Quantum Design MPMS-5T system with a measuring field of 20 G over the temperature range 5−50 K.

(15) Margadonna, S.; Brown, C. M.; Dennis, T. J. S.; Lappas, A.; Pattison, P.; Prassides, K.; Shinohara, H. *Chem. Mater.* **1998**, *10*, 1742−1744.

(16) Hino, S.; Matsumoto, K.; Hasegawa, S.; Kamiyama, K.; Inokuchi, H.; Morikawa, T.; Takahashi, T.; Seki, K.; Kikuchi, K.; Suzuki, S.; Ikemoto, I.; Achiba, Y. *Chem. Phys. Lett.* **1992**, *190*, 169−173.

(17) Dennis, T. J. S.; Kai, T.; Tomiyama, T.; Shinohara, H. *Chem. Commun.* **1998**, 619−620.

Results

X-ray Powder Diffraction. The X-ray powder diffraction patterns from both the D_{2d} and D_2 K_xC_{84} samples could be indexed as face-centered cubic unit cells with lattice parameters of 16.27(2) and 16.34(1) Å, respectively. LeBail integrated intensity fitting of the pattern proceeded smoothly to χ^2 values of 2.74 and 1.88. The data from the D_{2d} sample display a "foot" on the low-angle side of the 111 reflection, similar to that attributed to stacking faults in pure C_{60}, and the 200 reflection from a small quantity of KO_2 impurity at 15.8°. The 300 reflection of $K_2C_2O_6$ is visible in the diffraction pattern of D_2 K_xC_{84}. These impurities arise from reaction of small impurity gas concentrations in the drybox atmosphere with excess potassium condensed onto the $K_{8+x}C_{84}$ intermediate. The materials were both poorly crystalline with broad Bragg reflections and only diffracted out to 30° at 0.835 Å on the high signal-to-noise BM16 instrument, so the 30 integrated intensities limit the amount of quantitative information which can be extracted from the diffraction pattern. The observed cubic metric symmetry indicates that any total anion orientational order (which requires tetragonal and orthorhombic symmetry for the D_{2d} and D_2 isomers, respectively) is on a local scale and that on the diffraction length scale there is anion orientational disorder. The previous study of $K_{8+x}C_{84}$[13] demonstrated the correlation between the anion orientations and the resulting cation positions derived from analysis of the powder diffraction data: the cations can occupy not only the octahedral (O) and tetrahedral (T) positions familiar from the structure of K_3C_{60} but also *xxx* positions resulting from displacement away from the octahedral site center along the ⟨111⟩ directions to form a cube. The cubic metric symmetry of the solids means the C_{84} anions occupy positions of higher point symmetry ($m\bar{3}m$) than D_{2d} ($\bar{4}m2$) or D_2 (222), producing partial orientational disorder which can be minimized by aligning the normals to the mirror planes cutting through the 6:6 bonds of the molecules with the ⟨100⟩ directions ($\bar{4}m2$ symmetry) or along the ⟨110⟩ face diagonals ($\bar{4}2m$ symmetry) as detailed by Allen et al.[13]

D_{2d} K_xC_{84} Ambient-Temperature Diffraction. The initial refinements allowed potassium to occupy the O and T sites, and the fractional occupancies were refined together with the relative proportions of the anions in the ⟨100⟩ and ⟨110⟩ orientations, with temperature factors fixed at the values refined for $K_{8+x}C_{84}$. These refinements indicated 1.55(2) cations occupying the octahedral site, consistent with the presence of clusters on this site, while 60% of the anions adopted the ⟨110⟩ orientation. Subsequent refinements focused on developing chemically acceptable models for the excess scattering density on the octahedral site, constraining the models to prevent simultaneous occupation of the center and cube corner of an octahedral site. This is in accord with the refined compositions of the $K_{8+x}C_{84}$ phases, where the distances between the O site center and the corners of the *xxx* cubes demonstrated that either K_8 units or O site center K cations occupied the O sites in a mutually exclusive manner. These refinements (Figure 2) showed that all three (O, T, and cube corner sites) were partially occupied, and required the K···K distance within the cube to be constrained to be 3.60(1) Å to avoid unphysical contact distances. This resulted in a model with a refined composition of $K_{3.5(1)}C_{84}$ and the cation positions shown in Table 1.

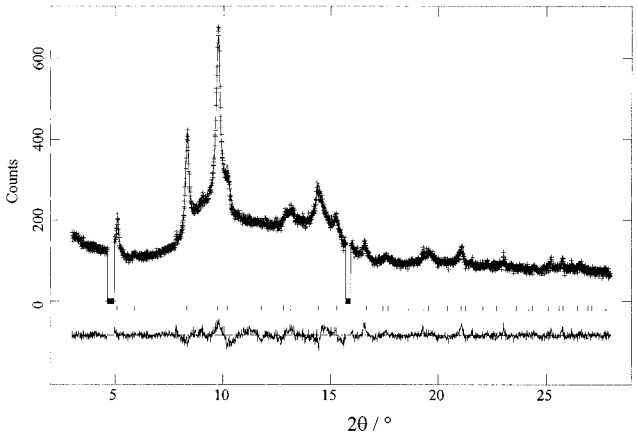

Figure 2. Rietveld refinement of X-ray powder diffraction data collected on the BM16 instrument at the ESRF from D_{2d} $K_{3.5(1)}C_{84}$. The observed data are points, the model is the solid line, and the difference is given at the bottom. The positions of the Bragg peaks are marked. The excluded region is due to the impurity KO_2 phase. $\chi^2 = 2.6$, and $R_e = 3.2\%$.

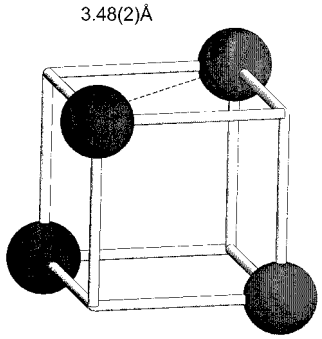

Figure 3. K_4 units occupying the octahedral site in D_{2d} $K_{3.5(1)}C_{84}$. The cations occupy the cube corner sites shown in Figure 1b in a disordered manner, but the refined distances prevent simultaneous occupation of adjacent cube vertexes, resulting in the tetrahedral local geometry shown here.

Table 1. Cation Positions, Occupancies, and Displacement Parameters for D_{2d} $K_{3.5(1)}C_{84}$ at 298 K[a]

x	*y*	*z*	U_{iso}/Å^2	fractional occupancy
0.25	0.25	0.25	0.01	0.542(13)
0.426(14)	0.426(14)	0.426(14)	0.03	0.240(7)
0.5	0.5	0.5	0.1	0.519(14)

[a] The anion positions are given in ref 11.

This model has K···K distances of 3.48(2) Å (Figure 3) within the tetrahedron (the cube edge is too short to allow simultaneous occupancy of neighboring, rather than diagonally opposed, positions on the cube cluster, as in Na_6C_{60}[18]) and K···C distances of between 3.080(2) and 3.480(2) Å to the ⟨110⟩ orientation of the C_{84} anion. Potassium cations occupy the centers of 51% of the O sites, while the remaining O sites are occupied by the K_4 tetrahedral units. These units are smaller than the K_8 cubes found in the saturated phases. The ⟨110⟩ anion orientation is 47(3)% occupied, while the remaining

(18) Rosseinsky, M. J.; Murphy, D. W.; Fleming, R. M.; Tycko, R.; Ramirez, A. P.; Siegrist, T.; Dabbagh, G.; Barrett, S. E. *Nature* **1992**, *356*, 416−418.

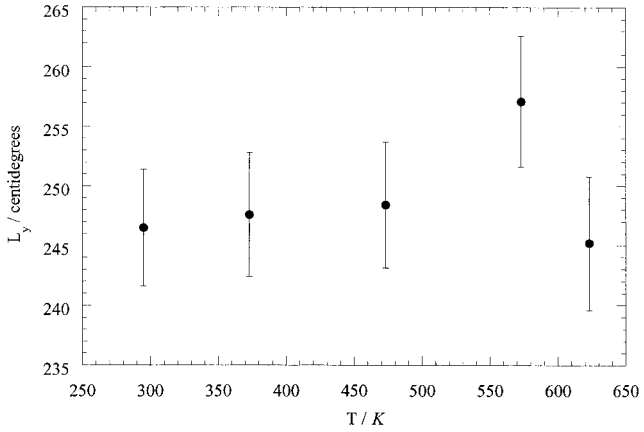

Figure 4. Variation of the parameter describing the Lorentzian peak width of the synchrotron X-ray powder diffraction pattern of D_{2d} $K_{3.5(1)}C_{84}$ with temperature.

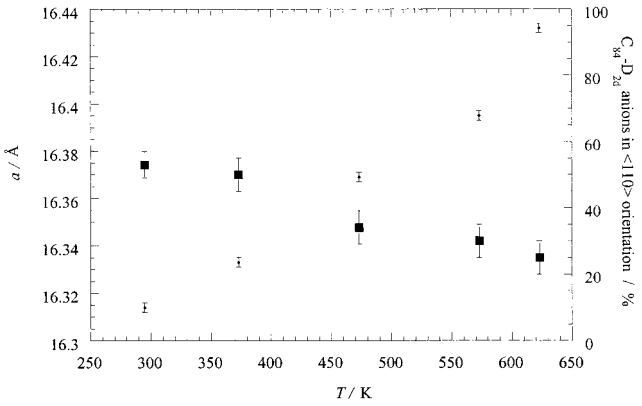

Figure 5. Temperature dependence of the cubic lattice parameter (circles) and fractional occupancy of the ⟨110⟩ orientation of the C_{84} anions (squares) in D_{2d} $K_{3.5(1)}C_{84}$, from refinement of synchrotron X-ray powder diffraction data.

53(3)% of the anions are aligned in the ⟨100⟩ orientation. This contrasts with the saturated $K_{8+x}C_{84}$ phases where the near-spherical disorder found for C_{84} itself is lost and the ⟨110⟩ orientation is exclusively adopted, to locate the potassium cation on the T site over the centroid of the hexagonal faces of the C_{84} anions. In the saturated phases, the tetrahedral site is 90% occupied, whereas in D_{2d} $K_{3.5(1)}C_{84}$ the occupancy is 54(1)%, which correlates well with the refined anion fractions in the two competing orientations. This shows the decisive effect of the tetrahedral cation on the anion orientations: without close contacts to intercalated cations, there is little tendency for orientational order, as shown by pristine C_{84}.[15] The heavily constrained analysis is required by the restricted angular range of the data, and the resulting models should be considered as such rather than as definitively refined structures. The constraints on the cation positions are needed to produce chemically acceptable K···K distances, which may reflect the actual existence of a variety of cation displacements from the octahedral site. This is plausible given the large size of this void in C_{84}, and the incomplete occupancy of the cube corner sites.

D_{2d} $K_{3.5(1)}C_{84}$ Variable-Temperature Diffraction. The width of the Bragg reflections at ambient temperature makes it impossible to rule out the existence of two or more closely related but distinct K_xC_{84} fcc phases. Temperature-dependent diffraction data were collected to distinguish this from the single-phase model via the different thermal expansions expected from different phases. Data at four temperatures up to 623 K were collected and refined with the same structural model as used at room temperature, and the peak widths as quantified by the refined Lorentzian L_y half-width parameter were constant within error over this temperature range (Figure 4). As at room temperature, it proved impossible to refine the atomic displacement parameters, and so the simple harmonic oscillator approximation to the cation displacements was used to scale the displacement parameters u from their room-temperature values (in the $k_BT \gg h\nu$ high-temperature limit $\langle u^2 \rangle = k_BT/h\nu$). The refined composition is temperature-independent, as are the cation distributions over the three available sites. The lattice parameter expansion on heating does however produce a significant change in the anion orientations, with the influence of the T cation favoring the ⟨110⟩ orientation being reduced by the thermal expansion to produce 75(5)% of the ⟨100⟩ orientation at 623 K (Figure 5). The observation that the refined cation site occupancies persist despite this change in orientation indicates that there are sufficient observations to decorrelate the anion orientations from the cation distribution, and that the salient features of the structural model derived at room temperature are robust.

Table 2. Cation Positions, Occupancies, and Displacement Parameters for D_{2d} $K_{2.6(1)}C_{84}$ at 298 K[a]

x	*y*	*z*	U_{iso}/Å^2	fractional occupancy
0.25	0.25	0.25	0.01	0.277(13)
0.4229(3)	0.4229(3)	0.4229(3)	0.03	0.181(8)
0.5	0.5	0.5	0.1	0.665(16)

[a] The anion positions are given in ref 11.

D_2 $K_{2.6(1)}C_{84}$. As in the D_{2d} case, trial refinements indicated an excess of potassium on the O site ($\chi^2 = 1.9$ for 1.2 cations per O site). The refined site occupancies and positional parameters of the cations again indicated a mixture of O center cations and K_4 tetrahedral clusters on the O sites, with a K−K distance-constrained refinement yielding a composition of D_2 $K_{2.6(1)}C_{84}$ with 33.5% of the O sites occupied by the K_4 tetrahedron with a 3.57(4) Å separation. A 79(4)% fraction of the anions are aligned with the ⟨110⟩ orientation, compared with 68% of the D_2 molecules in D_2 $K_{7.92}C_{84}$ (Figure 6 and Table 2). The temperature-dependent studies also showed the absence of significant peak broadening on heating and a robust overall composition and cation site occupancy, the major difference from the D_{2d} phase being that the ⟨110⟩ population remained roughly constant with temperature. The data collected on station 9.1 for this phase were of poorer statistical quality than those for $K_{3.5(1)}C_{84}$ and relatively insensitive to anion orientation, so this difference may not be significant. The variable-temperature data for this phase are given as Supporting Information.

EPR Spectroscopy. *D_{2d} $K_{3.5(1)}C_{84}$*. At all temperatures the EPR spectra can be fitted to a single Lorentzian signal, consistent with the single-phase interpretation of the powder diffraction data. The g value of 2.0021 is close to the free-electron value, indicating

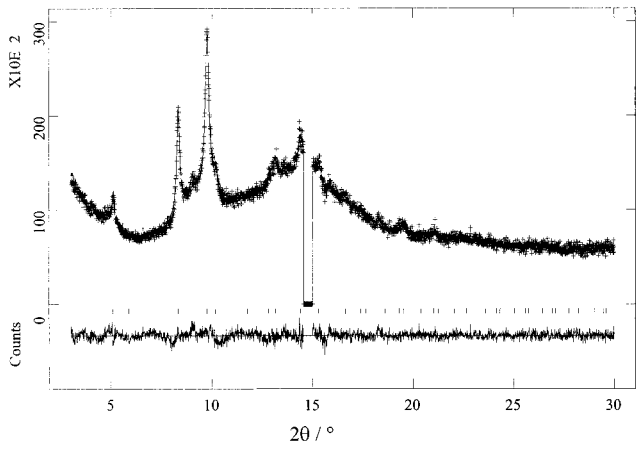

Figure 6. Rietveld refinement of X-ray powder diffraction data from D_2 $K_{2.6(1)}C_{84}$ collected on the BM16 instrument at the ESRF. The observed data are points, the model is the solid line, and the difference is given at the bottom. The positions of the Bragg peaks are marked. The excluded region is due to the impurity $K_2C_2O_6$ phase. $\chi^2 = 1.6$, and $R_w = 2.9\%$.

carbon-based spins consistent with complete charge transfer to C_{84} from the K^+ cations, but was not determined with sufficient precision to distinguish between the 2− and 3− charge states. The line shape of D_{2d} C_{84}^{2-} is characterized by a 13 G zero-field splitting characteristic of a triplet state,[19] and the absence of this is consistent with the presence of 3− anions indicated by Rietveld refinement.

The EPR susceptibility (Figure 7a) has a temperature dependence quite different from that of the K-saturated D_{2d} $K_{8+x}C_{84}$ phase, with a small effective magnetic moment of 0.22 μ_B per fullerene and a Weiss constant of 3.5 K, equal to 0.024 unpaired electrons per C_{60} and attributed to localized paramagnetic defects. The dominant contribution to the susceptibility is a temperature-independent term of 1.3×10^{-4} emu mol^{-1}, and the most straightforward interpretation of this is as the Pauli susceptibility of a metallic phase, with a density of states at the Fermi energy of 2.01 states eV^{-1} C_{84}^{-1} $spin^{-1}$. In a metal in which the electron−phonon scattering rate $1/\tau$ is proportional to temperature, the Elliot relationship[20] between T_1 and τ predicts that $\Delta H/(\Delta g)^2$ should be linear in the temperature (where ΔH is the EPR line width, $\Delta g = g - g_e$, and g_e is the free-electron g value), and this has been observed for A_3C_{60} phases.[21] Due to the proximity of the g value to g_e, the errors on Δg are large at high temperature, but a linear relationship can be established at low temperature and seen to persist into the less well-defined higher temperature region (Figure 7b). The scattering rate $1/\tau$ depends on a proportionality constant α, which is not well-known in fulleride systems.

D_2 $K_{2.7(1)}C_{84}$. As in the D_{2d} case, the EPR data are fitted at all temperatures with a single Lorentzian, consistent with the presence of a single paramagnetic phase indicated by the X-ray data. D_2 C_{84}^{2-} is observed to be EPR silent,[19] and the g value of 2.002(1) is

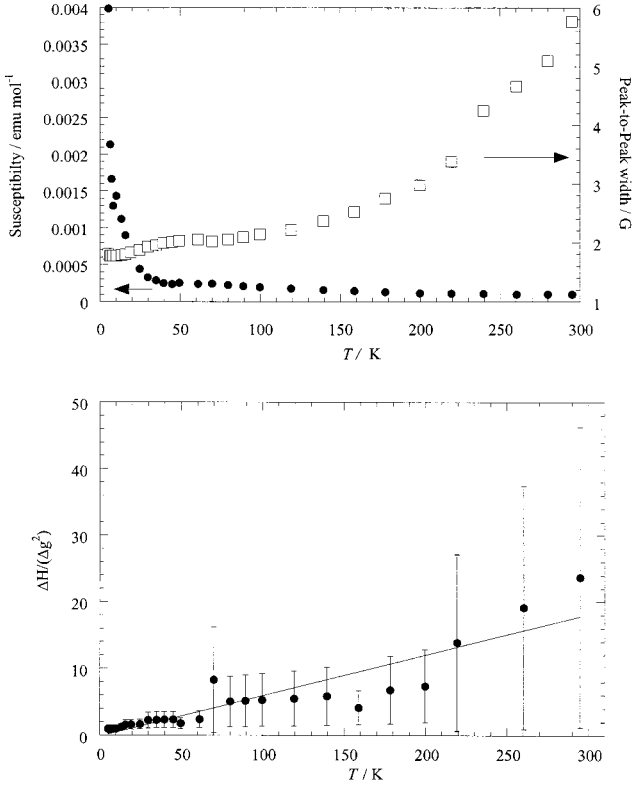

Figure 7. (a, top) Peak-to-peak line width (G; squares) and magnetic susceptibility (emu mol^{-1}; circles) from EPR measurements on D_{2d} $K_{3.5(1)}C_{84}$. (b, bottom) Temperature dependence of the EPR line width normalized to the g value variation ($\Delta H/(\Delta g)^2$) of D_{2d} $K_{3.5(1)}C_{84}$. This function is linear in a metal above its Debye temperature.

consistent with solution measurements of the D_{2d} C_{84}^{3-} anion. The susceptibility (Figure 8a) consists of a small Curie−Weiss component ($\Theta = 1.86$ K, $m = 0.49$ μ_B/C_{84}) corresponding to 0.114 unpaired spins per C_{84}, plus the temperature-independent component of 1.7×10^{-4} emu mol^{-1}, corresponding to a density of states at the Fermi level of 2.63 states eV^{-1} C_{84}^{-1} $spin^{-1}$. The dependence of $\Delta H/(\Delta g)^2$ upon temperature (Figure 8b) is consistent with the interpretation of this as the Pauli susceptibility of a metal, although the small value of Δg leads again to large errors in this quantity at high temperature.

Although the EPR intensity and line width indicate that both D_{2d} $K_{3.5(1)}C_{84}$ and D_2 $K_{2.7(1)}C_{84}$ are metallic, the low-field SQUID magnetization data indicate that neither sample is superconducting above 5 K.

Discussion

The synchrotron X-ray diffraction data and EPR data presented here indicate that a phase of stoichiometry $K_{3+x}C_{84}$ can be prepared for both D_{2d} and D_2 C_{84} isomers. The EPR data show there is only one paramagnetic phase per sample, while the monotonic lattice parameter variation with temperature and the absence of anomalies in the refined peak widths together with the robustness of the structural models are all consistent with the single-phase hypothesis. This is consistent with potassium 2p X-ray photoemission studies of mixed-isomer K_xC_{84} phases, which suggest the formation of a phase with composition K_3C_{84}.[22] The refined stoichiometry of these phases does not correspond to the target

(19) Boulas, P. L.; Jones, M. T.; Ruoff, R. S.; Lorents, D. C.; Malhotra, R.; Tse, D. S.; Kadish, K. M. *J. Phys. Chem.* **1996**, *100*, 7573−7579.
(20) Elliott, R. J. *Phys. Rev.* **1954**, *96*, 266−287.
(21) Petit, P.; Robert, J.; Yildrim, T.; Fischer, J. E. *Phys. Rev. B* **1996**, *54*, R3764−R3767.

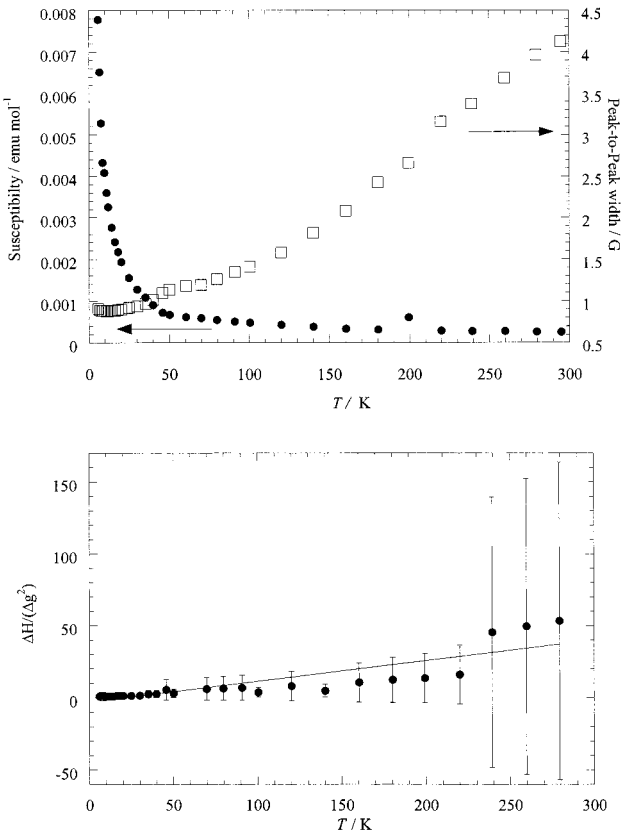

Figure 8. (a, top) Peak-to-peak line width (G; squares) and magnetic susceptibility (emu mol^{-1}; circles) from EPR measurements on D_2 $K_{2.6(1)}C_{84}$. (b, bottom) Temperature dependence of $\Delta H/(\Delta g)^2$ of D_2 $K_{2.6(1)}C_{84}$. This function is linear in a metal above its Debye temperature.

stoichiometry of K_2C_{84}. There is no evidence in the diffraction pattern for unreacted C_{84}, implying that an excess of potassium was present in the reaction mixture. The small amount of C_{84} available makes accurate control of the stoichiometry very difficult, and this is an important area for future work.

The Rietveld refinements indicate considerable differences in the extent of anion ordering between the potassium-saturated phases and the phases synthesized here. For D_{2d} $K_{8+x}C_{84}$ the anions are exclusively aligned with the normals to the molecular mirror planes along the ⟨110⟩ directions of the unit cell. For D_{2d} $K_{3.5(1)}C_{84}$ only 47(3)% of the anions are set in this orientation, presumably because of the lower fractional occupancy of the tetrahedral site by potassium.

The refinements are consistent with tetrahedral metal units on the octahedral site for the compounds of both isomers. This can be deduced from the site occupancies using chemically sensible limits on the minimum K···K distances.

The inter-potassium separations in body-centered cubic (bcc) potassium metal are 4.54 and 4.2 Å in K-loaded zeolite A,[23] whereas the contact distances of 3.631(2) Å in the K_8 cubes in $K_{8+x}C_{84}$ are shorter. In the present tetrahedral K_4 clusters, the K···K separations are 3.48 and 3.57 Å, similar to those in the K_8 cubes. The K_4 units implied here are considerably smaller than the K_8 cubes however because the closest contacts referred to above would be face diagonals of the K_8 cubes. This, combined with the reduced occupancy of the tetrahedral sites compared to the saturated phases, means that the intercalated cations in the present case interact considerably less strongly with the fulleride anions and consequently exert less of an orientationally ordering influence. This extreme disorder may be important in determining both sample crystallinity and electronic properties.

In D_{2d} $K_{3.5(1)}C_{84}$, only 47(3)% of the anions adopt the ⟨110⟩ orientation exclusively favored in D_{2d} $K_{8+x}C_{84}$. In D_2 $K_{2.6(1)}C_{84}$, 79(4)% of the anions are aligned in the ⟨110⟩ orientation favored by contacts to the T cation, suggesting that the D_2 isomer is more strongly affected orientationally by contacts to the intercalated cations. As described by Allen et al.,[13] the ⟨110⟩ orientation locates the six-membered rings of the D_{2d} and D_2 isomers over the tetrahedral and cube corner cations and minimizes potentially unfavorable close K···C contacts. For both orientations, the 3-fold axis in $Fm\bar{3}m$ imposes an orientational disorder on the fulleride anions as neither the D_2 C_{84} nor the D_{2d} C_{84} molecule has a 3-fold axis. The partial occupancy of the interstitial sites also implies a considerable amount of cation site disorder, and the large size of the octahedral site compared with C_{60} suggests static and dynamic displacements will be more pronounced compared with those of A_3C_{60} phases. This, coupled with the intrinsic narrow bandwidth of the fullerides, may have serious implications for whether a metallic ground state is observed. The disorder may reduce the one-electron bandwidth to an extent where Mott−Hubbard localization occurs, or it may manifest itself in Anderson localization of some of the electrons. The density of states (DOS) in an Anderson-localized insulator is finite, and thus χ_{CESR} would be independent of temperature as observed.

The observed temperature-independent components in the ESR susceptibility data indicate that the samples both are metallic or at least have a nonzero density of states at the Fermi energy. The temperature-independent component of the susceptibility is directly proportional to the densities of states at the Fermi energy, which are 2.01 and 2.6 states eV^{-1} C_{84}^{-1} spin^{-1} for the D_{2d} and D_2 isomers, respectively. The linear dependence of $\Delta H/(\Delta g)^2$ for the D_2 isomer provides supporting evidence for the metallic nature of this phase. The nonlinear temperature dependence of the line width for the D_{2d} isomer may be due to a change in the scattering mechanism of the conduction electrons with temperature or a structural phase transition.

The precise location of the Fermi level in the two phases studied here depends on the composition, which is not well-determined. The D_{2d} LUMO is doubly degenerate, and the LUMO-derived band in D_{2d} $K_{3.5(1)}C_{84}$ is thus approximately 75% full. This is comparable to the 4− (66%) and 5− (83% filling of the t_{1u} band) charge C_{60}-based fullerides. The pronounced influence of the precise band filling is shown by the contrasting semiconducting and metallic behavior of K_4C_{60}[24] and Ba_2CsC_{60},[25] respectively, and demonstrates that the band

(22) Poirier, D. M.; Weaver, J. H.; Kikuchi, K.; Achiba, Y. *Z. Phys. D: At., Mol. Clusters* **1993**, *26*, 79−83.

(23) Woodall, L. J.; Anderson, P. A.; Armstrong, A. R.; Edwards, P. P. *J. Chem. Soc., Dalton Trans.* **1996**, 719.

(24) Kerkoud, R.; Auban-Senzier, P.; Jerome, D.; Lambert, J. M.; Zahab, A.; Bernier, P. *Europhys. Lett.* **1994**, *25*, 379−384.

filling in the D_{2d} C_{84} case at least is compatible with metallic behavior. The pronounced structural disorder in both isomer-pure C_{84} phases would be expected to produce significant energy broadening and density-of-states reduction in such systems where the small near-neighbor transfer integrals will be particularly sensitive to local disorder. For D_{2d} $K_{3.5(1)}C_{84}$, the value of the density of states at the Fermi level of 2.01 states eV^{-1} C_{84}^{-1} $spin^{-1}$ is N_χ, enhanced over the bare value N_b by electron−electron correlation effects. This is quantitatively accounted for by the Stoner parameter I via eq 1,

$$1/N_b = 1/N_\chi + I \quad (1)$$

where $I = 0.03$ spin eV C_{60} in A_3C_{60} systems.[26] If we assume that I is transferable to the C_{84}-based systems studied here, then N_b is reduced to 1.9 states eV^{-1} C_{84}^{-1} $spin^{-1}$, considerably reduced from 7.7 states eV^{-1} C_{84}^{-1} $spin^{-1}$ found for K_3C_{60}. As the superconducting transition temperature can be modeled according to the McMillan equation[27] (eq 2), we can scale $\lambda = VN_b$ from

$$k_B T_c = \frac{\hbar\omega_{ph}}{1.2} \exp\left[\frac{-1.04(1+\lambda)}{\lambda - \mu^*(1+0.62\lambda)}\right] \quad (2)$$

$\lambda = 1.2$ of K_3C_{60} using the ratios of the measured N_b values, and (assuming that the value of the Coulomb repulsion parameter μ^* is 0.3) this leads to the denominator of eq 2 becoming unphysically small as the weakened electron−phonon coupling no longer competes with the electron−electron repulsion. Although this is a necessarily qualitative argument, it does give an explanation for the absence of superconductivity in the C_{84}-based phases studied here. Theoretical estimates[12] indicate that this suppression of T_c by the reduced N_b will actually be compounded by a reduction in V, the electron−phonon deformation potential, on going from C_{60} to the less curved C_{84} due to the reduced s hybridization of the π orbitals. The conduction electron scattering rate can in principle be extracted from the gradient of the $(\Delta H)/(\Delta g)^2$ plot,[21] which is linear for a metal above its Debye temperature, but depends on a quantity α not well-determined for fullerides: use of the value estimated for A_3C_{60} phases of $\alpha = 0.005$ yields $\tau^{-1} = 3.4 \times 10^{16}$ s^{-1}, higher than found for the better-ordered A_3C_{60} phases. This may indicate that interpretation in terms of an Anderson-localized insulator is to be preferred.

Conclusion

The compositions of both C_{84} salts are close to those of the A_3C_{60} superconductors, in which the alkali-metal cations occupy the octahedral and tetrahedral sites completely and produce (for A = K, Rb) a line phase composition where the insertion of further cations requires a change of sphere packing to body-centered (body-centered tetragonal A_4C_{60} and cubic A_6C_{60}). The larger interstitial sites in C_{84} produce a quite different intercalation chemistry more reminiscent of the Na_xC_{60} phases, with multiple cation occupancy of the O site producing cube-related cation groups coexisting with or substituting for the O site center cation familiar from K_3C_{60}. This flexibility of the O site occupancy allows the composition to vary smoothly across the fcc K_xC_{84} phase field.

The absence of superconductivity in K_xC_{84} can be attributed to the extensive anion orientational and cation positional disorder; the precise influence of anion orientations on fulleride physical properties has been shown by the paramagnetic and ferromagnetic TDAE-C_{60} phases differing only in their anion orientations.[28] It is of course possible, given the extreme sensitivity of fulleride properties to anion charge, that the anion charges in the present two phases cannot support superconductivity. Future studies should focus on more precise compositional control and the use of larger alkali-metal cations, which will reduce the positional disorder when they occupy the spacious O site.

Acknowledgment. We thank the Leverhulme Trust and the EPSRC (Grant GR/M04006) for supporting this work, and Dr. A. Fitch and Dr. M. A. Roberts for assistance at the ESRF and Daresbury facilities, respectively.

Supporting Information Available: Figures showing the variation of the parameter describing the Lorentzian peak width of the synchrotron X-ray powder diffraction pattern of D_2 $K_{2.6(1)}C_{84}$ with temperature and the temperature dependence of the cubic lattice parameter and fractional occupancy of the ⟨110⟩ orientation of the C_{84} anions in D_2 $K_{2.6(1)}C_{84}$ (PDF). This material is available free of charge via the Internet at http://pubs.acs.org.

CM010595C

(25) Thier, K. F.; Goze, C.; Mehring, M.; Rachdi, F.; Yildirim, T.; Fischer, J. E. *Phys. Rev. B* **1999**, *59*, 10536.
(26) Robert, J.; Petit, P.; Yildirim, T.; Fischer, J. E. *Phys. Rev. B* **1998**, *57*, 1226−1231.
(27) McMillan, W. L. *Phys. Rev.* **1968**, *167*, 331.
(28) Narymbetov, B.; Omerzu, A.; Kabanov, V. V.; Tokumoto, M.; Kobayashi, H.; Mihailovic, D. *Nature* **2000**, *407*, 883−885.